Differential function of *Listeria monocytogenes* listeriolysin O and phospholipases C in vacuolar dissolution following cell-to-cell spread

Christine Alberti-Segui,* Kathryn R. Goeden and Darren E. Higgins*

Department of Microbiology and Molecular Genetics, Harvard Medical School, Boston, MA 02115, USA.

Summary

We investigated the role of listeriolysin O (LLO) and the bacterial phospholipases PI-PLC and PC-PLC in cell-to-cell spread of *Listeria monocytogenes*. We showed that LLO is essential for cell-to-cell spread in primary murine macrophages. Electron micrographs revealed that in the absence of continued LLO expression, bacteria remain trapped in secondary spreading vacuoles having either a double or single membrane. In bacteria lacking PI-PLC and PC-PLC, cessation of LLO expression after initiation of infection resulted in a significant increase in the proportion of bacteria trapped in double-membrane compartments. We propose that the bacterial phospholipases are involved in the dissolution of the inner membrane of the spreading vacuole, yet are not sufficient for disruption of the outer membrane. As a consequence, we identified LLO as a key factor in the disruption of the outer membrane. This model is consistent with the observation that LLO is dispensable for cell-to-cell spread from human macrophages into a cell type in which LLO is not required for vacuolar escape. These data suggest that during human infection, spreading of *L. monocytogenes* to distant organs is likely to occur even in the absence of LLO expression, and that the bacterial phospholipases may be sufficient to mediate continued cell-to-cell spread.

Introduction

Listeria monocytogenes is a Gram-positive, facultative intracellular bacterium that is an important food-borne pathogen. *L. monocytogenes* causes serious and often fatal infections in humans, particularly in immunocompro-

mised individuals, pregnant women and neonates (Lorber, 1997; Vazquez-Boland *et al.*, 2001). Bacteria have the ability to invade a wide variety of cells including professional phagocytes (e.g. macrophages and dendritic cells) (Mackaness, 1962; Pron *et al.*, 2001), and non-professional phagocytic cells such as fibroblasts (Kuhn *et al.*, 1988), hepatocytes (Dramsi *et al.*, 1995), neurons (Dramsi *et al.*, 1998), endothelial cells (Drevets *et al.*, 1995) and epithelial cells (Gaillard *et al.*, 1987). Host cell invasion occurs by phagocytosis or pathogen-induced endocytosis in non-professional phagocytic cells (Gaillard *et al.*, 1987). In addition to direct invasion, tissue infection can occur through cell-to-cell spread of bacteria from an infected host cell into an alternative cell type (e.g. heterologous spreading). In particular, cell-to-cell spread from circulating infected phagocytes to distant tissues is currently thought to be an important step in the establishment of systemic infection (Drevets, 1999; 2001; Drevets and Leenen, 2000; Pron *et al.*, 2001; Join-Lambert *et al.*, 2005). Spreading from macrophages to alternative cell types has also been demonstrated *in vitro* (Drevets *et al.*, 1995; Dramsi *et al.*, 1998; Greiffenberg *et al.*, 1998). Considering the importance of heterologous spreading in the progression of infection, a better understanding of heterologous cell-to-cell spread is of considerable interest for the development of strategies to prevent systemic infection.

At the cellular level, cell-to-cell spread can be divided into three stages: (i) actin-based motility and filopod formation, (ii) bacterial uptake and formation of the double-membrane spreading vacuole and (iii) membrane dissolution. Several studies have contributed to understanding the molecular mechanism underlying *L. monocytogenes* cell-to-cell spread. On the host side, the Arp2/3 complex, one of the two major actin nucleating activities in cells, plays a central role in *L. monocytogenes* intracellular motility (Cossart, 2000), thereby facilitating intercellular spread (Gouin *et al.*, 2005). Inhibition studies have revealed a role for phosphoinositide-3-kinase in actin-based motility and ultimately in filopod formation (Sidhu *et al.*, 2005). Finally, ezrin, a member of the ezrin, radixin and moesin family that functions as a key membrane-cytoskeleton linker, has been recently implicated in formation and stabilization of filopods (Pust *et al.*, 2005). Bacterial determinants of cell-to-cell spread have

also been identified. These include the bacterial surface protein ActA, involved in actin-based motility (Cossart, 2000), and three secreted bacterial factors that are known to interact with host cell membranes and contribute to vacuolar lysis: listeriolysin O (LLO), a pore-forming cytolysin (Portnoy *et al.*, 1988; Gedde *et al.*, 2000; Dancz *et al.*, 2002), and two membrane-active phospholipases C, a broad range phospholipase C (PC-PLC) and a phosphatidylinositol-specific phospholipase C (PI-PLC) (Camilli *et al.*, 1991; 1993; Vazquez-Boland *et al.*, 1992; Smith *et al.*, 1995). At two distinct stages during the infection process bacteria are surrounded by vacuolar membranes. Upon entry, bacteria are trapped within single-membrane vacuoles. Failure to escape from these primary vacuoles results in an abortive and avirulent infection. In contrast, by gaining access to the cytosol, bacteria can replicate and spread to adjacent cells. Following spreading, bacteria are trapped within double-membrane vacuoles. Escape from these secondary spreading vacuoles is again critical for intracellular replication and the establishment of a successful infection. LLO assisted by PI-PLC mediates membrane disruption of the single-membrane primary vacuole (Gaillard *et al.*, 1987; Camilli *et al.*, 1993; Smith *et al.*, 1995). In the secondary vacuole, efficient dissolution of the double-membrane requires all three membrane-active factors (Vazquez-Boland *et al.*, 1992; Smith *et al.*, 1995). Interestingly, in some human cell lines, LLO has been shown to be dispensable for vacuolar lysis and a major role for PC-PLC in membrane dissolution of primary and secondary vacuoles in the absence of LLO has been recently recognized (Portnoy *et al.*, 1988; Marquis *et al.*, 1995; Gründling *et al.*, 2003).

Our understanding of the function of LLO in cell-to-cell spread is a result of studies examining spread of *L. monocytogenes* between identical cell types (e.g. homologous spreading). Recently, LLO has been identified as a key factor in the degradation of the double-membrane spreading vacuole in J774 murine macrophage-like cells (Gedde *et al.*, 2000). To overcome the absolute requirement of LLO expression for primary vacuolar lysis in J774 cells, Gedde *et al.* used purified LLO coupled to LLO-negative bacteria. In the absence of expression of the bacterial phospholipases and LLO, bacteria were able to spread to neighbouring J774 cells, but remained trapped within multiple-membrane compartments (Gedde *et al.*, 2000). Although technically challenging, this approach allowed the study of cell-to-cell spread in the absence of LLO expression. Using a genetic approach based on a previously described inducible expression system (Dancz *et al.*, 2002), we have investigated the role of LLO and the two bacterial phospholipases for cell-to-cell spread of *L. monocytogenes* in murine bone marrow-derived macrophages (mBMDM).

We have shown that in primary murine macrophages, LLO, PI-PLC and PC-PLC act to disrupt double-membrane vacuoles formed upon intercellular spreading. However, unlike in J774 cells, cessation of LLO expression in the absence of the two phospholipases resulted in a majority of bacteria remaining trapped in secondary vacuoles that consisted of no more than two membranes. Interestingly, following intercellular spread of bacteria lacking both phospholipases, yet expressing LLO, multiple membranes reminiscent of those described for autophagy were observed. In addition, data presented in this report suggest that in mBMDM, PI-PLC and PC-PLC facilitate membrane disruption by specifically acting on the inner membrane of the spreading vacuole and that LLO is absolutely required for the degradation of the outer membrane. Supporting this model, we show that bacterial phospholipases are sufficient to trigger escape from the double-membrane compartments formed upon cell-to-cell spread from human macrophages to human epithelial cells, the latter cell type being one in which LLO is dispensable for vacuole escape. Thus, our findings question the absolute requirement of LLO expression during systemic human infection.

Results

In vitro *and* in vivo *characterization of an improved inducible LLO strain*

Listeriolysin O has been shown to be absolutely required for vacuolar escape in all mouse-derived cells tested (Portnoy *et al.*, 1988; Vazquez-Boland *et al.*, 2001). In these cells, LLO-negative mutants remain trapped within primary vacuoles, therefore rendering difficult the study of the role of LLO in the subsequent stages of infection. To study the role of LLO in cell-to-cell spread, we decided to construct a regulated promoter that would allow tight control of LLO expression. In a prior study (Dancz *et al.*, 2002), the *hly* gene (encoding LLO) was successfully placed under the control of an inducible promoter that was based on the *Escherichia coli lac* operator/repressor system. The expression construct contained the *Bacillus subtilis* phage SPO-1 promoter adjacent to a single ideal *lac* operator site (*lac*Oid). The SPAC/*lac*Oid-inducible promoter allowed efficient inducible control of LLO expression and the study of the temporal requirement of LLO during intracellular infection. However, the SPAC/*lac*Oid-inducible promoter was not stringently repressed in the absence of the inducer (isopropyl-β-D-thiogalactopyranoside, IPTG). To ensure tight repression of gene expression, we introduced a second *lac*Oid repressor binding site upstream of the SPO-1 promoter region. Binding of the LacI repressor as a homotetramer to both operator sites simultaneously was expected to occur through the formation of a DNA loop and would efficiently
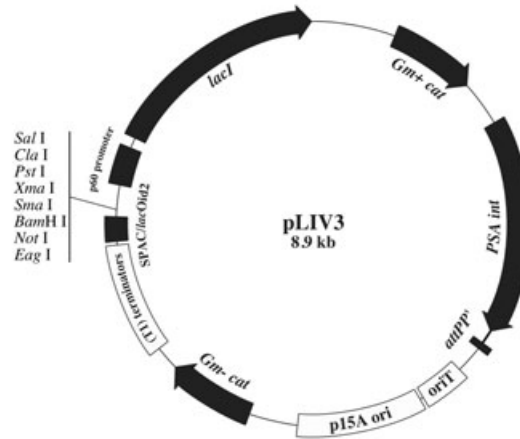
Fig. 1. Inducible expression vector for conditional repression studies in *L. monocytogenes*.
A. Plasmid map of pLIV3. The IPTG-inducible promoter (SPAC/*lac*Oid2) is followed by a multiple cloning site that consists of eight unique restriction sites that can be used for cloning. The *L. monocytogenes* p60 promoter ensures constitutive expression of the *lac* repressor gene (*lacI*). Other determinants on the pLIV3 plasmid are identical to those found on the site-specific phage integration vector pPL2 (Lauer *et al*., 2002). *cat*, chloramphenicol resistance gene for selection in Gram-positive (Gm+ *cat*) or Gram-negative (Gm– *cat*) bacteria; (p15A ori), *E. coli* origin of replication; (oriT), origin of transfer to allow conjugal mating of plasmid from *E. coli* to *L. monocytogenes*; (PSA *int*), PSA integrase gene; (*att*PP′), PSA phage attachment site; (T1 terminators), tandem copies of the *rrn*B T1 transcription terminator.
B. Nucleotide sequence of the SPAC/*lac*Oid2-inducible promoter within pLIV3. The −35 and −10 regions are overlined with the transcription initiation site (+1) noted. The *lac*Oid operator sequences are boxed. Restriction sites used to clone the promoter/operator region are noted and underlined.

repress transcription from the SPO-1 promoter (Oehler *et al.*, 1994). The resulting inducible promoter consisting of the SPO-1 promoter flanked by two *E. coli lac*Oid operator sequences (SPAC/*lac*Oid2) was incorporated into a site-specific phage integration vector, yielding plasmid pLIV3 (Fig. 1). The *hly* gene was placed under the transcriptional control of the SPAC/*lac*Oid2 promoter/operator in pLIV3 and the resulting vector integrated into the chromosome of an LLO-negative *L. monocytogenes* strain to generate the inducible LLO (iLLO) strain DH-L1239. As shown in Table 1, in the absence of IPTG, no haemolytic activity (HU) was detected in the supernatant of cultures of the iLLO strain, indicating that LLO expression was tightly repressed. Only upon addition of IPTG was haemolytic activity detected in culture supernatants, indicating that LLO was produced and secreted. Haemolytic activity increased with increasing concentrations of IPTG with a maximum of 36.2 HU observed at an IPTG concentration of 10 mM (Table 1). No increase in haemolytic activity was observed at IPTG concentrations above 10 mM (data not

shown). Therefore, even under maximal IPTG induction, the haemolytic activity observed with the iLLO strain represented approximately 33% of wild-type strain 10403S (Table 1). Consistent with the haemolytic activity data, the

Table 1. Haemolytic activity.[a]

Strains	IPTG (mM)	Haemolytic units [HU (± SD)]
10403S	0	109.2 (± 18.03)
iLLO	0	n.d.
	0.1	16.7 (± 1.5)
	0.25	24.7 (± 1.6)
	0.5	28.4 (± 3.6)
	1	30.9 (± 0.9)
	10	36.2 (± 2.8)

a. A 16 h culture of iLLO strain DH-L1239 was diluted 1:10 in BHI medium and grown for 5 h at 37°C in the presence of various concentrations of IPTG. Wild-type strain 10403S was grown under similar conditions in the absence of IPTG. Haemolytic activity present in culture supernatants was determined as described in *Experimental procedures*. HU values represent the means and standard deviations (± SD) of three independent experiments. n.d., not detected.
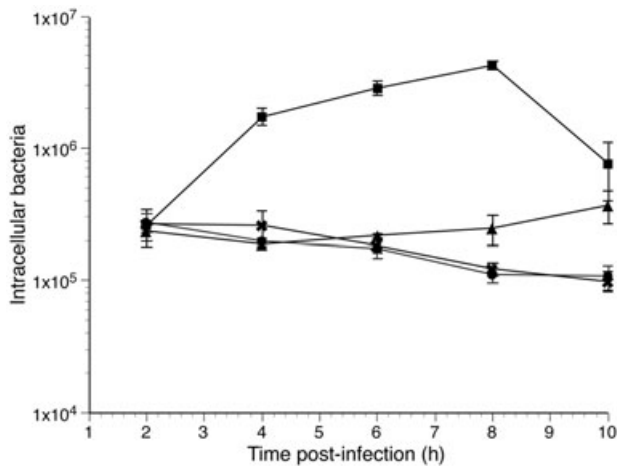
Fig. 2. Intracellular growth of the DH-L1239 iLLO strain in mBMDM. Sixteen-hour cultures of *L. monocytogenes* strains were diluted 1:10 in BHI medium in the presence or absence of IPTG and grown for 2 h at 37°C. Monolayers of mBMDM were infected at a moi of 10:1 (bacteria per host cell ratio) with wild-type (10403S; squares), LLO-negative (DP-L2161; circles) or iLLO bacteria (DH-L1239) maintained in the presence (triangles) or absence (X) of IPTG. For induction of iLLO bacteria, IPTG was added to BHI medium at a concentration of 0.5 mM and maintained during infection of mBMDM at a concentration of 10 mM. At the indicated time points post infection, the number of intracellular bacteria was determined as described in *Experimental procedures*. Data shown represent the means ± SD of one of three independent experiments performed in triplicate with similar results.

iLLO strain in the absence of IPTG failed to escape primary vacuoles in mBMDM and was therefore unable to initiate intracellular replication (Fig. 2). However, in the presence of IPTG several foci of infection were observed by microscopy (data not shown), indicating that under inducing conditions iLLO bacteria were able to escape primary vacuoles. Nonetheless, only 2% of iLLO bacteria successfully escaped the vacuolar compartment in mBMDM compared with 70% for wild-type bacteria (data not shown). This inefficient vacuolar escape is consistent with the observation that even under full IPTG induction intracellular infection by iLLO bacteria in mBMDM was less efficient than wild-type bacteria (Fig. 2). Taken together, these data indicated that although well repressed, the SPAC/*lac*Oid2 promoter could not be induced to produce LLO to a level similar to wild-type bacteria. However, the DH-L1239 iLLO strain was stringently repressed in the absence of inducer. Therefore, the DH-L1239 strain is more suitable for studies of LLO function that require stringent conditional repression of LLO production.

Listeriolysin O is required to escape the secondary vacuole during cell-to-cell spread between mBMDM

Listeriolysin O has been shown to be required for escape from double-membrane spreading vacuoles in J774

murine macrophage-like cells (Gedde *et al.*, 2000). To determine whether LLO is also required for cell-to-cell spread in primary murine macrophages, iLLO bacteria grown in the presence of IPTG (pre-induced) were used to infect a monolayer of CellTracker™ Blue-labelled mBMDM in the absence of inducer. In the absence of continued IPTG induction, we speculated that intracellular LLO production would cease (Table 1). At 6 h post infection, the infected mBMDM were added to a secondary monolayer of unlabelled mBMDM in the absence of IPTG. At 4 h post secondary cell infection, cell monolayers were processed for fluorescence microscopy and analysed for cell-to-cell spreading events. The majority of the primary infected mBMDM contained multiple bacteria. However, approximately 10% of these CellTracker™ Blue-labelled cells were heavily infected with bacteria associated with F-actin (Fig. 3A, iLLO no IPTG). These data suggested that only a few iLLO bacteria were successful in escaping primary vacuoles under these conditions, a result consistent with decreased haemolytic activity and a low frequency of vacuolar escape by the iLLO strain compared with wild type (Table 1 and data not shown). In addition, we frequently observed bacteria in secondary host cells located adjacent to heavily infected CellTracker™ Blue-labelled cells. We hypothesized that these bacteria were the result of cell-to-cell spread from the primary infected CellTracker™ Blue-labelled mBMDM into secondary cells. To confirm that these bacteria were the result of cell-to-cell spread and not due to lysis of primary infected mBMDM and subsequent phagocytosis by secondary mBMDM, we performed a similar infection using iLLO bacteria containing an in-frame deletion in the *actA* gene. Deletion of the *actA* gene has been shown to prevent actin-based motility and cell-to-cell spread of *L. monocytogenes* (Mounier *et al.*, 1990; Domann *et al.*, 1992; Kocks *et al.*, 1992; Sanger *et al.*, 1992). If the presence of iLLO bacteria in secondary mBMDM was due to cell-to-cell spread, then bacteria should not be found in secondary cells using the Δ*actA* iLLO strain. Infection of mBMDM with pre-induced Δ*actA* iLLO bacteria resulted in the formation of large bacterial aggregates frequently located around the nucleus in CellTracker™ Blue-labelled mBMDM (Fig. 3A, Δ*actA* iLLO). Secondary host cells were completely devoid of Δ*actA* iLLO bacteria, indicating that the presence of iLLO bacteria in secondary cells was a consequence of cell-to-cell spread.

In a similar analysis of cell-to-cell spread, infection of mBMDM with wild-type bacteria also resulted in the presence of bacteria in secondary host cells (Fig. 3A, wild-type). However, the majority of bacteria in secondary host cells were associated with F-actin. These results indicated that wild-type bacteria successfully spread into adjacent host cells and subsequently escaped from the spreading vacuole before initiating continued intracellular replication
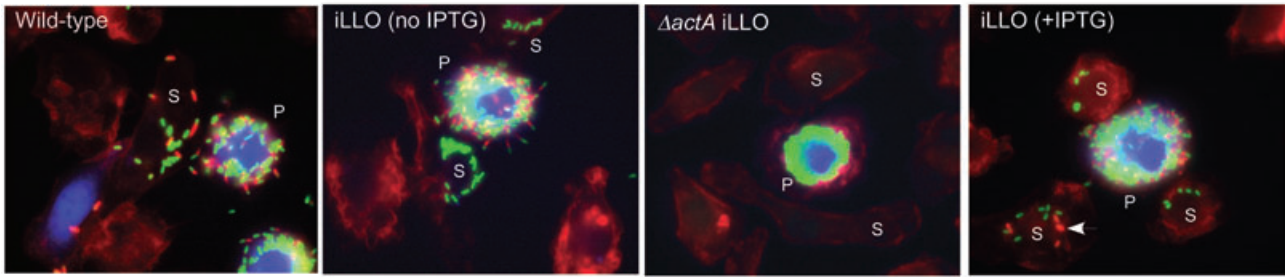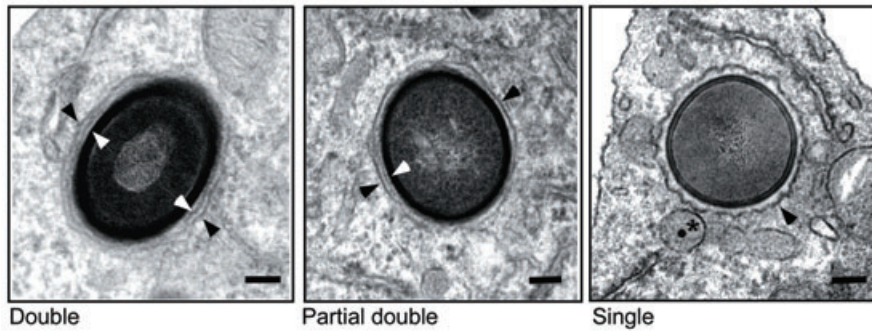
Fig. 3. Cessation of LLO expression during infection of mBMDM results in bacteria remaining trapped within secondary spreading vacuoles. iLLO bacteria pre-induced with IPTG prior to infection were used to infect monolayers of CellTracker™ Blue-labelled mBMDM at a moi of 30:1 in the absence of IPTG. At 6 h post infection, infected host cells (primary infection) were added to a monolayer of uninfected, non-labelled mBMDM and incubated for an additional 4 h (secondary infection). Monolayers were then fixed and stained for F-actin and *L. monocytogenes*. A. Fluorescence microscopy. Primary infected host cells (P) are labelled in blue, bacteria in green and F-actin in red. Secondary host cells (S). Shown is a representative image from one of two experiments for each strain. At least 50 foci of infection were examined for each strain per experiment with similar results. Wild-type *L. monocytogenes* and ΔactA iLLO were used as controls. For iLLO bacteria, secondary infection was performed in the absence (no IPTG) or presence of 10 mM IPTG (+IPTG). Arrow in the iLLO (+IPTG) panel indicates bacteria associated with F-actin in a secondary host cell.
B. Electron micrographs of iLLO bacteria in secondary host cells. Electron microscopy experiments were performed as described in *Experimental procedures*. Single black arrows indicate a single membrane; a pair of black and white arrows indicates a double membrane with the white arrow immediately adjacent to the inner membrane and the black arrow immediately adjacent to the outer membrane. The asterisk indicates a 20 nm colloidal gold bead used to specifically label and identify secondary host cells. Scale bars = 100 nm.

and actin-based motility. In contrast to wild-type bacteria, iLLO bacteria found in secondary cells were not associated with F-actin (Fig. 3A, iLLO no IPTG). These results suggested that in the absence of continued LLO expression, iLLO bacteria were able to enter secondary cells via cell-to-cell spread, but failed to escape the spreading vacuole.

Transmission electron microscopy confirmed that in the absence of continued LLO expression, iLLO bacteria present in secondary host cells were trapped in vacuolar compartments. These compartments consisted of a double, partial double (presence of regions of double and single membranes around the same bacterium) or single membrane (Fig. 3B). Quantitative analysis of the membrane organization of spreading vacuoles showed that a majority (60 ± 10.0%) of the iLLO bacteria were trapped in single-membrane compartments (Table 2). To confirm that the cell-to-cell spread arrest was caused by the absence of LLO expression, we performed a similar infection in which IPTG was added during the secondary infection. Under these conditions, iLLO bacteria retained the ability to escape from secondary spreading vacuoles, as indicated by the association of F-actin with bacteria in secondary host cells (Fig. 3A, iLLO + IPTG). Taken together, these data suggest that LLO is not required for pseudopod formation and uptake by adjacent cells, but is critical for escape from the double-membrane secondary vacuole formed upon cell-to-cell spread between primary macrophages.

The L. monocytogenes *phospholipases contribute to cell-to-cell spread in mBMDM by facilitating escape from secondary vacuoles*

In the absence of the two phospholipases, LLO has been shown to mediate escape from primary and secondary vacuoles in murine L2 fibroblasts (Smith *et al.*, 1995). However, infection of L2 cell monolayers with a PLC-negative strain during plaquing assays resulted in a decrease in plaque size that was interpreted as a defect in

Table 2. Membrane organization of the vacuolar compartments formed upon cell-to-cell spread of *L. monocytogenes* in mBMDM.[a]

Strains	Double[b]	Partial double[c]	Single[d]
iLLO	**15.6% (± 5.1)**	**24.4% (± 7.7)**	**60.0% (± 10.0)***
Exp. 1	1/6 (16.7%)	2/6 (33.3%)	3/6 (50.0%)
Exp. 2	1/5 (20.0%)	1/5 (20.0%)	3/5 (60.0%)
Exp. 3	1/10 (10.0%)	2/10 (20.0%)	7/10 (70.0%)
ΔPLCs iLLO	**77.4% (± 21.5)**	**8.9% (± 7.8)**	**13.7% (± 14.3)***
Exp. 1	6/8 (75.0%)	1/8 (12.5%)	1/8 (12.5%)
Exp. 2	7/7 (100%)	0/7 (0%)	0/7 (0%)
Exp. 3	4/7 (57.1%)	1/7 (14.3%)	2/7 (28.6%)
ΔPI-PLC iLLO	**14.6% (± 2.9)**	**32.3% (± 1.5)**	**53.1% (± 4.4)***
Exp. 1	2/12 (16.7%)	4/12 (33.3%)	6/12 (50.0%)
Exp. 2	2/16 (12.5%)	5/16 (31.2%)	9/16 (56.3%)
ΔPC-PLC iLLO	**13.2% (± 3.0)**	**34.9% (± 5.8)**	**51.9% (± 2.7)***
Exp. 1	2/13 (15.4%)	4/13 (30.8%)	7/13 (53.8%)
Exp. 2	2/18 (11.1%)	7/18 (38.9%)	9/18 (50.0%)

Strain names and % values representing the mean of two to three experiments are shown in bold.
*Represents a statistically significant difference between the value given and the value listed in the 'Double' category as determined by the Student's *t*-test ($P < 0.02$).
a. Summary of electron microscopy results presented in Fig. 3 (iLLO) and Fig. 5 (ΔPLCs iLLO). In addition, the table includes electron microscopy results obtained with strains ΔPI-PLC iLLO and ΔPC-PLC iLLO. % values are the mean (± SD) of two to three experiments with the results from each individual experiment given.
b. Proportion of bacteria in secondary cells surrounded by an intact double-membrane vacuole.
c. Proportion of bacteria in secondary cells surrounded by a partial double-membrane vacuole.
d. Proportion of bacteria in secondary cells surrounded by a single-membrane vacuole.

secondary vacuolar escape. To determine whether LLO is sufficient to mediate secondary vacuolar escape in mBMDM and to evaluate the contribution of the two phospholipases in cell-to-cell spread, we analysed the ability of PLC-negative bacteria to spread from cell-to-cell using a similar approach as described for the iLLO strain. Quantitative fluorescence microscopy studies showed that more than 50% of wild-type bacteria in secondary Cell-Tracker™ Blue-labelled cells were associated with F-actin at 4 h post secondary infection (Fig. 4A and Table 3). A majority of these bacteria had polymerized actin tails. In contrast, only 15% of PLC-negative bacteria in secondary cells were associated with F-actin (Fig. 4A and Table 3). Out of 170 actin-associated PLC-negative bacteria in secondary cells, only seven harboured actin tails. These data suggested that during the 4 h secondary infection period very few PLC-negative bacteria were successful in escaping secondary spreading vacuoles to continue infection.

Transmission electron microscopy confirmed that at 4 h post secondary infection, a minority (20.3%) of PLC-negative bacteria were free in the cytosol of secondary cells (Fig. 4B, EM5 and Table 3). The remaining 79.7% of bacteria were surrounded by membranes (Fig. 4B, EM1–4 and Table 3), with a majority (76%) of bacteria trapped in double or multiple membrane compartments (EM1, 2, 4). Occasionally, bacteria were associated with multilamelar compartments or 'onion-like membranous structures' (Fig. 4B, EM3) that were reminiscent of those described for autophagy (Hernandez *et al.*, 2003; Agaisse *et al.*, 2005; Ogawa *et al.*, 2005). These multiple membrane compartments were not observed during infection with wild-type bacteria. Altogether, these data suggest

that in the absence of the two phospholipases, bacteria are partially defective in secondary vacuolar escape and may become targets of autophagy. We concluded that the two phospholipases are not essential for cell-to-cell spread in mBMDM, but appear to be required for efficient dissolution of the spreading vacuole.

The bacterial phospholipases function in the dissolution of the inner membrane of mBMDM spreading vacuoles

Inducible LLO bacteria trapped in mBMDM secondary vacuoles (Fig. 3B) still retain the ability to express PI-PLC and PC-PLC. To determine the effect of the loss of phospholipase expression on the membrane organization of the secondary vacuole, we constructed an iLLO strain lacking expression of both PI-PLC and PC-PLC. The resulting strain (ΔPLCs iLLO) showed similar *in vitro* LLO induction as the iLLO strain (Table 1 and data not shown). Analysis of cell-to-cell spread in mBMDM using pre-induced ΔPLCs iLLO bacteria resulted in very few primary infected host cells containing actively growing bacteria (Fig. 5A). This is consistent with a role for PI-PLC in synergizing with LLO to facilitate escape from primary vacuoles (Smith *et al.*, 1995). Nonetheless, the presence of ΔPLCs iLLO bacteria in secondary cells adjacent to primary infected host cells containing numerous bacteria indicated successful cell-to-cell spreading events. Similar to our results with iLLO (Fig. 3, iLLO no IPTG), none of the ΔPLCs iLLO bacteria in secondary cells were associated with F-actin (Fig. 5A). Transmission electron microscopy revealed that bacteria in secondary mBMDM were also trapped in vacuolar compartments (Fig. 5B). In contrast to
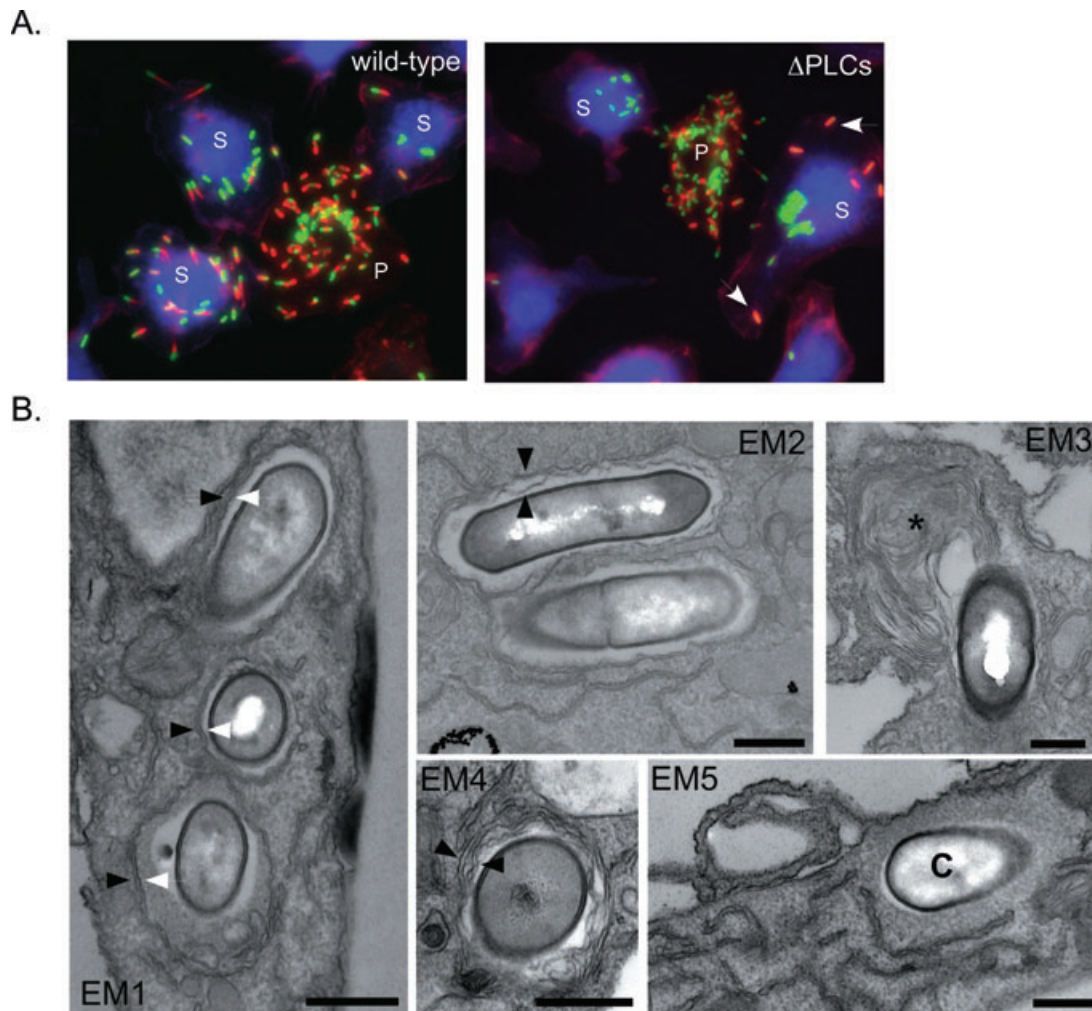
Fig. 4. PI-PLC-, PC-PLC-negative *L. monocytogenes* are partially defective in secondary vacuolar escape during infection of mBMDM. Wild-type or PLC-negative bacteria were used to infect non-labelled mBMDM at a moi of 5:1. At 3 h post infection, infected host cells (primary infection) were added to a monolayer of uninfected, CellTracker™ Blue-labelled mBMDM, and incubated for an additional 4 h (secondary infection). Monolayers were then fixed and processed for fluorescence and electron microscopy.
A. Fluorescence microscopy. Secondary host cells (S) are labelled in blue, bacteria in green and F-actin in red. Primary infected host cells (P). Shown is a representative image from one of three experiments for each strain. At total of 30 foci of infection were examined for each strain with similar results. Arrows in the PLC-negative panel (ΔPLCs) indicate bacteria associated with F-actin in a secondary host cell.
B. Electron micrographs of PLC-negative bacteria in secondary host cells. Arrows and arrowheads indicate membranes surrounding bacteria. A pair of black and white arrows indicates a double membrane. A pair of black arrowheads indicates the presence of multiple membranes. The asterisk indicates a multilamelar structure associated with the bacterium. Panel EM5 depicts a cytosolic bacterium (C). Scale bars = 500 nm.

iLLO bacteria, the majority of ΔPLCs iLLO bacteria in secondary cells (77.4 ± 21.5%) were found surrounded by a double membrane (Table 2). Taken together, these data suggested that the membrane organization of the secondary vacuole formed upon cell-to-cell spread in the absence of LLO expression is dependent upon the presence or absence of the *L. monocytogenes* phospholipases. In the presence of PI-PLC and PC-PLC, the majority of the bacteria (60%) were trapped in single-membrane compartments, while in absence of both phospholipases, bacteria were predominantly (77.4%) surrounded by a double membrane (Table 2). We concluded from these data that *L. monocytogenes* PI-PLC

and PC-PLC could specifically facilitate the dissolution of the inner membrane of the spreading vacuole in primary murine macrophages.

Either PI-PLC or PC-PLC can mediate dissolution of the inner membrane of mBMDM spreading vacuoles

To determine whether the dissolution of the inner membrane of mBMDM spreading vacuoles was due to one or both of the phospholipases, we generated iLLO strains that express either one or the other phospholipase (ΔPI-PLC iLLO expressing PC-PLC and ΔPC-PLC iLLO expressing PI-PLC). Interestingly, cell-to-cell spread fol-

Table 3. Secondary vacuolar escape in mBMDM.[a]

Strain (genotype)	Fluorescence microscopy[b] % bacteria in secondary cells staining with phalloidin at 4 h post secondary infection (mean ± SD)	Electron microscopy[c]	
		% bacteria in the cytosol of secondary cells*	% bacteria in secondary cells surrounded by membrane(s)**
10403S (wild-type)	54.7 ± 3.6 (377/687)	57.7 ± 22.6 (24/43)	42.3 ± 22.6 (19/43)
DP-L1936 (ΔPLCs)	15.0 ± 5.8 (170/1250)	20.3 ± 16.5 (10/48)	79.7 ± 16.5 (38/48)

*Number of bacteria in the cytosol/total number of bacteria observed in secondary cells.
**Number of bacteria surrounded by membranes/total number of bacteria observed in secondary cells.
a. Summary of fluorescence and electron microscopy results presented in Fig. 4.
b. % values are the mean (± SD) of three experiments. A total of 30 foci of infection were analysed for each strain. The total number of bacteria from the three experiments that associated with actin/total number of bacteria observed in secondary cells for each strain is indicated in parentheses.
c. % values are the mean (± SD) of two experiments. The results from the sum of the two experiments is given in parentheses.

lowing cessation of LLO expression resulted in a majority of bacteria (~50%) remaining trapped in single-membrane compartments during infection of mBMDM by both ΔPI-PLC iLLO and ΔPC-PLC iLLO bacteria (Table 2). Furthermore, 32–35% of ΔPI-PLC iLLO or ΔPC-PLC iLLO bacteria were found in partial double-membrane compartments. These data suggest that in mBMDM, either PI-PLC or PC-PLC can act on the inner membrane of the spreading vacuole to mediate dissolution, yet LLO is required to degrade/perforate the outer membrane of the spreading vacuole to facilitate vacuolar escape.

Listeriolysin O is dispensable for cell-to-cell spread between human-derived macrophages and epithelial cells

Our data indicate that LLO is absolutely required for the dissolution of the outer membrane of spreading vacuoles in mBMDM. Therefore, we speculated that in the absence of continued LLO expression, bacteria that spread into a cell type for which LLO is not required for vacuolar lysis would escape from secondary vacuoles. We analysed cell-to-cell spread from U937 human-derived macrophages into human Hep2 epithelial cells using a modified plaquing assay (heterologous plaquing). We chose Hep2 cells as recipient cells as they are permissive for vacuolar escape and intracellular growth of LLO-negative bacteria (Gründling *et al.*, 2003). U937 cells were infected with pre-induced iLLO bacteria in the absence of IPTG. iLLO-infected U937 cells were then cocultured with a monolayer of Hep2 cells in the presence of gentamicin. The ability of iLLO bacteria to escape heterologous spreading vacuoles in Hep2 cells and continue intracellular infection was monitored by the formation of plaques in Hep2 cell monolayers. To discard the possibility that plaques formed were the result of lysis of infected U937 cells and subsequent uptake of iLLO bacteria by Hep2 cells, we determined: (i) the frequency of plaques formed when Hep2

cell monolayers were infected directly with wild-type bacteria in the presence of gentamicin and (ii) the frequency of plaques formed when Hep2 cells were infected in the presence of gentamicin with iLLO bacteria released from primary infected U937 cells (U937 lysate). As shown in Fig. 6, 31 ± 7 (*n* = 4) plaques were obtained when iLLO-infected U937 cells were used to initiate infection of Hep2 cells, whereas only a few plaques (2 ± 2; *n* = 4) were detected with direct infection of the Hep2 cell monolayer with wild-type bacteria in the presence of gentamicin (Fig. 6E). This result together with the observation that no plaques were formed in control experiments using U937 lysate (Fig. 6F) suggested that the majority of plaques obtained with iLLO-infected U937 cells were the result of efficient cell-to-cell spread between infected macrophages and Hep2 cells, followed by subsequent cell-to-cell spread between Hep2 cells. Therefore, iLLO bacteria in the absence of continued LLO expression escaped heterologous double-membrane vacuoles comprised of an U937-derived inner membrane and a Hep2-derived outer membrane. As expected, infection with iLLO bacteria lacking expression of PI-PLC and PC-PLC (ΔPLCs iLLO strain) resulted in no plaques being formed in the heterologous plaquing assay (Fig. 6B). In addition, Hep2 cells were overlaid with U937 cells infected with ΔPI-PLC iLLO bacteria, a strain that is capable of forming plaques during direct infection of Hep2 cell monolayers. Interestingly, no plaques were observed (Fig. 6C). Taken together, these data suggest that following initiation of intracellular infection, LLO is dispensable for cell-to-cell spread between human macrophages and human epithelial cells and that both PI-PLC and PC-PLC are required to mediate escape from heterologous double-membrane spreading vacuoles in the absence of LLO expression.

Discussion

Cell-to-cell spread of *L. monocytogenes* is complete when bacteria escape double-membrane vacuoles formed upon

spreading into adjacent cells. In this report, we identified LLO as a key factor for the dissolution of double-membrane spreading vacuoles in mBMDM. Using a tightly regulated inducible expression system, we demonstrated that following initiation of infection, cessation of LLO expression in primary infected cells resulted in an abortive phenotype with bacteria remaining trapped in secondary spreading vacuoles (Fig. 3). A specific requirement of LLO for escape of secondary vacuoles has also been reported in J774 macrophages (Gedde *et al.*, 2000). Similarly, transient expression of LLO during infection of L2 fibroblasts resulted in the formation of pinpoint plaques that were interpreted as being due to the inability of bacteria to escape secondary vacuoles (Dancz *et al.*, 2002). Therefore, LLO appears to be essential for the dissolution of secondary spreading vacuoles in murine-derived cells.

In addition to LLO, *L. monocytogenes* secretes two phospholipases, PI-PLC and PC-PLC, that are known to interact with host cell membranes and contribute to the lysis of vacuolar compartments during infection (Vazquez-Boland *et al.*, 1992; Camilli *et al.*, 1993; Smith *et al.*, 1995). Results presented here indicate that the bacterial phospholipases contribute to cell-to-cell spread in mBMDM by facilitating escape from secondary spreading vacuoles. This is in agreement with the observation that infection of murine L2 fibroblasts with PLC-negative bacteria results in small plaques (Smith *et al.*, 1995) and supports a general role for *L. monocytogenes* phospholipases in cell-to-cell spread between murine cells. Interestingly, consistent with a considerable reduction in secondary vacuolar escape efficiency, a significant proportion of the PLC-negative bacteria were trapped in double or multiple membrane compartments that were reminiscent of those described for autophagy (Hernandez *et al.*, 2003; Agaisse *et al.*, 2005; Ogawa *et al.*, 2005). Nonetheless, multilamelar structures were not observed around bacteria after cessation of LLO expression (Figs 3 and 5). Our findings suggest that *L. monocytogenes* or possibly LLO-damaged vacuoles are becoming targets of autophagy and support the recent findings by Birmingham *et al.* that intracellular pathogens exposed to the cytosol through perforations or gaps within phagocytic vacuoles induce autophagy (Birmingham *et al.*, 2006). Taken together, these data suggest that *L. monocytogenes* has to express LLO and the phospholipases to efficiently dissolve the double-membrane spreading vacuole and evade host-cell defence mechanisms (e.g. autophagy).

In the absence of continuous LLO expression, cell-to-cell spread in primary mBMDM resulted in the majority of bacteria remaining trapped within single-membrane vacuolar compartments (Table 2). Only a few examples (15.6%) of bacteria surrounded by a double membrane were observed. We hypothesized that in the absence of LLO, the inner membrane of the spreading vacuole is degraded

due to the activity of the bacterial phospholipases. Indeed, we found that in the absence of PI-PLC and PC-PLC expression, a significant increase in the proportion of bacteria trapped in double-membrane compartments following cell-to-cell spread was observed (Table 2, ΔPLCs iLLO strain). Based on these data, we propose that during cell-to-cell spread in murine-derived cells PI-PLC and PC-PLC participate in dissolution of the inner membrane of the spreading vacuole, yet LLO is responsible for facilitating dissolution of the outer membrane. In addition, in the absence of LLO expression, the majority of bacteria lacking either PI-PLC or PC-PLC remained trapped in single-membrane spreading compartments (Table 2), suggesting that both phospholipases can facilitate dissolution of the inner membrane of the spreading vacuole. The modest increase in the proportion of bacteria surrounded by a partial double-membrane (Table 2; ΔPI-PLC iLLO or ΔPC-PLC iLLO compared iLLO bacteria) might be due to slower membrane dissolution kinetics in the presence of one as compared with both phospholipases. A model for PI-PLC and PC-PLC acting synergistically to dissolve secondary vacuoles is in agreement with previous reports suggesting an overlapping function for *L. monocytogenes* phospholipases in promoting cell-to-cell spread (Smith *et al.*, 1995). Moreover, assuming that membrane phospholipid composition in murine macrophages follows the general features of phospholipid asymmetry in eukaryotic cells (Zwaal *et al.*, 1975; Calderon and DeVries, 1997), the inner leaflet of the membrane closest to bacteria after spreading is expected to be rich in phosphatidylethanolamine (PE), phosphatidylserine (PS) and phosphatidylinositol (PI) (Fig. 7A). As PE and PS are good substrates for PC-PLC (Goldfine *et al.*, 1993; Montes *et al.*, 2004) and PI is the major substrate for PI-PLC (Goldfine and Knob, 1992), it is plausible that both PI-PLC and PC-PLC act synergistically on the inner membrane of the spreading vacuole.

In the absence of the two phospholipases, a small proportion of iLLO bacteria were found in single-membrane compartments (Table 2, ΔPLCs iLLO). One possibility is that these bacteria were derived from lysis of primary infected cells and subsequent phagocytosis by secondary cells. Although our studies demonstrated that primary infected cell lysis contributes minimally (Fig. 3A, ΔactA iLLO), we cannot rule out the possibility for occasional cell lysis during the secondary infection process. In addition, preliminary studies on the fate of bacteria trapped in secondary vacuoles revealed that vacuolar compartments are ultimately targeted to the lysosomal degradation pathway (data not shown) as indicated by the presence of the late-endosomal marker LAMP-1 (Pitt *et al.*, 1992; Beron *et al.*, 1995; Gruenberg and Maxfield, 1995). Therefore, the presence of single-membrane spreading vacuoles surrounding iLLO bacteria lacking
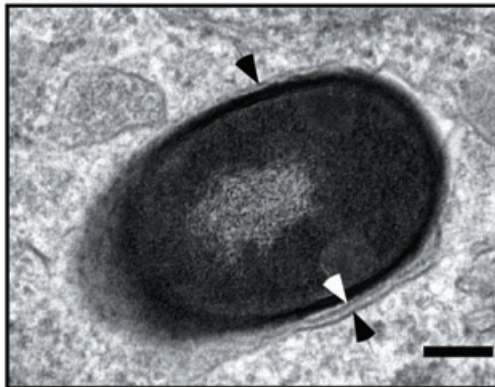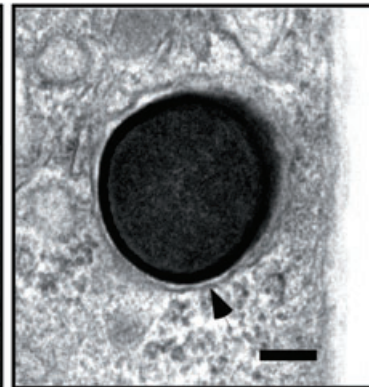
A.
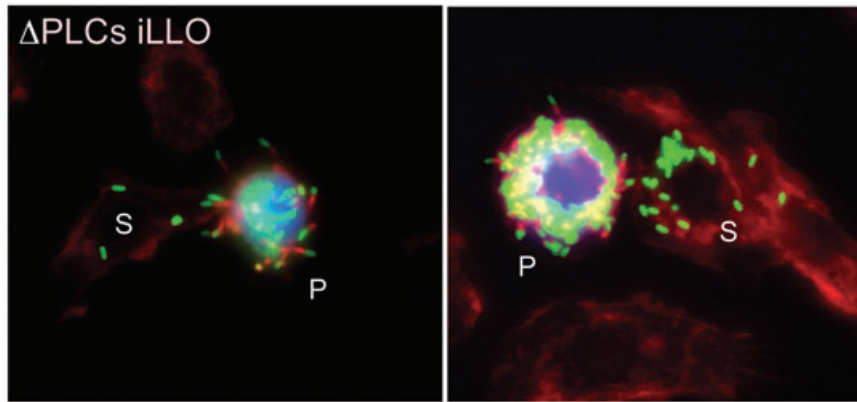
B.
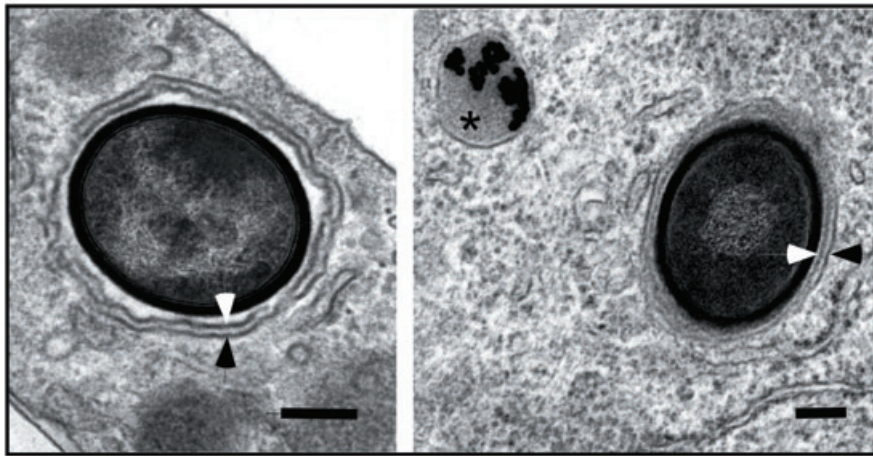
Double

Partial double

Single

PI-PLC and PC-PLC expression is more likely due to a fusion event with lysosomal compartments.

From our studies, it is not clear whether phospholipase-mediated disappearance of the inner membrane of spreading vacuoles is the result of membrane disruption and/or a membrane fusion event. A membrane fusion activity has been recently described for PC-PLC (Montes *et al.*, 2004). It is possible that membrane fusion induced by PC-PLC is one of the mechanisms that contribute to the dissolution of the double-membrane spreading vacuole. Indeed, the simultaneous presence of double and single membranes (partial double) surrounding bac-

Fig. 5. The *L. monocytogenes* phospholipases function in the dissolution of the inner membrane of mBMDM spreading vacuoles. ∆PLCs iLLO bacteria grown in BHI medium were pre-induced with IPTG prior to infection of CellTracker™ Blue-labelled mBMDM. Infection of mBMDM was performed at a moi of 30:1 in the absence of IPTG. At 6 h post infection, infected host cells (primary infection) were added to a monolayer of uninfected, non-labelled mBMDM and incubated for an additional 4 h (secondary infection). Monolayers were then fixed and stained for F-actin and *L. monocytogenes*.
A. Fluorescence microscopy. Primary infected host cells (P) are labelled in blue, bacteria in green and F-actin in red. Secondary host cells (S). Shown are two representative foci of infection from one of two experiments. At least 50 foci of infection were examined for each experiment with similar results.
B. Electron micrographs of ∆PLCs iLLO bacteria in secondary host cells. Electron microscopy experiments were performed as described in *Experimental procedures*. Single black arrows indicate a single membrane; a pair of black and white arrows indicates a double membrane with the white arrow immediately adjacent to the inner membrane and the black arrow immediately adjacent to the outer membrane. The asterisk indicates an aggregate of 20 nm colloidal gold beads that were used to label secondary host cells. Scale bars = 100 nm.

teria in secondary cells could be interpreted as a snap shot of a fusion event between the two membranes of the vacuolar compartment.

After disappearance of the inner membrane, the bacterium faces the outer leaflet of the outer membrane. Again, following the general features of phospholipid asymmetry in eukaryotes, the outer leaflet is thought to be rich in phosphatidylcholine (PC) and sphingomyelin (Sph) (Fig. 7A). Several experiments have shown that PC and Sph can also be substrates for PC-PLC (Geoffroy *et al.*, 1991; Goldfine *et al.*, 1993; Montes *et al.*, 2004). Therefore, in theory PC-PLC should be able to attack not only the inner membrane, but also the outer membrane of the spreading vacuole. However, in the presence of PC-PLC alone, bacteria did not escape sec-

ondary vacuoles, suggesting that PC-PLC activity is restricted to the inner membrane. Using large unilamelar liposomes of defined composition, it was recently shown that PS-, PE-rich vesicles are better substrates for PC-PLC than PC-, Sph-rich vesicles (Montes *et al.*, 2004). Therefore, it is possible that PC-PLC activity towards the outer membrane of spreading vacuoles is inefficient in triggering membrane dissolution before vacuoles become acidified. We are currently investigating whether the overexpression of PC-PLC in the presence of an inhibitor of vacuole acidification alleviates the inability of PC-PLC to degrade the outer membrane of mBMDM spreading vacuoles.

When the outer membrane of the spreading vacuole was derived from a cell type for which LLO is not required
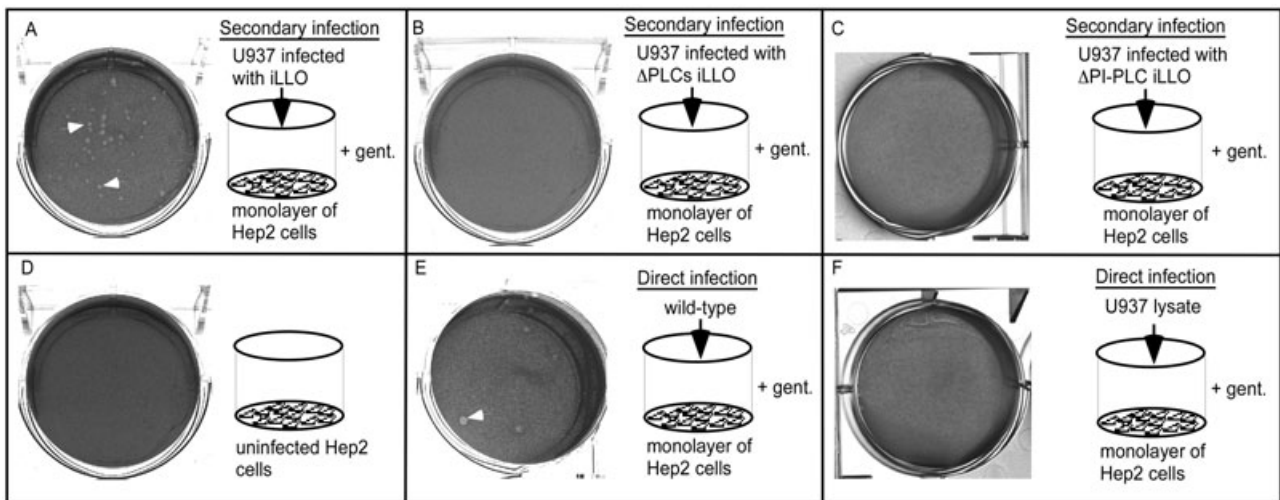

Fig. 6. LLO is dispensable for cell-to-cell spread between human-derived macrophages and human epithelial cells. Human-derived U937 macrophages were infected in the absence of IPTG with pre-induced iLLO, ∆PLCs iLLO or ∆PI-PLC iLLO bacteria at a moi of 50:1. At 6 h post infection, infected U937 macrophages were added to monolayers of Hep2 epithelial cells at a moi of 2:3 (primary to secondary host cell ratio) in the presence of gentamicin and in the absence of IPTG (secondary infection). Monolayers were overlaid 3 h post secondary infection with an agarose medium mixture containing gentamicin without IPTG. Plaques within the monolayers were visualized 5–6 days post secondary infection.
A. Heterologous plaquing assay with iLLO bacteria. A total of 4×10^5 infected U937 (representing a total of $1–2 \times 10^6$ bacteria) were used to infect a monolayer of Hep2 cells. Arrows point to representative plaques. Each plaque is the result of a successful heterologous cell-to-cell spread event followed by subsequent cell-to-cell spreading and Hep2 cell lysis.
B. Heterologous plaquing assay with ∆PLCs iLLO bacteria.
C. Heterologous plaquing assay with ∆PI-PLC iLLO bacteria.
D. Monolayers of Hep2 cells were left uninfected.
E. A total of 1.25×10^8 wild-type bacteria were added directly to Hep2 cells in the presence of gentamicin.
F. U937 lysate (representing a total of $1–2 \times 10^6$ iLLO bacteria) were added directly to Hep2 cells in the presence of gentamicin.
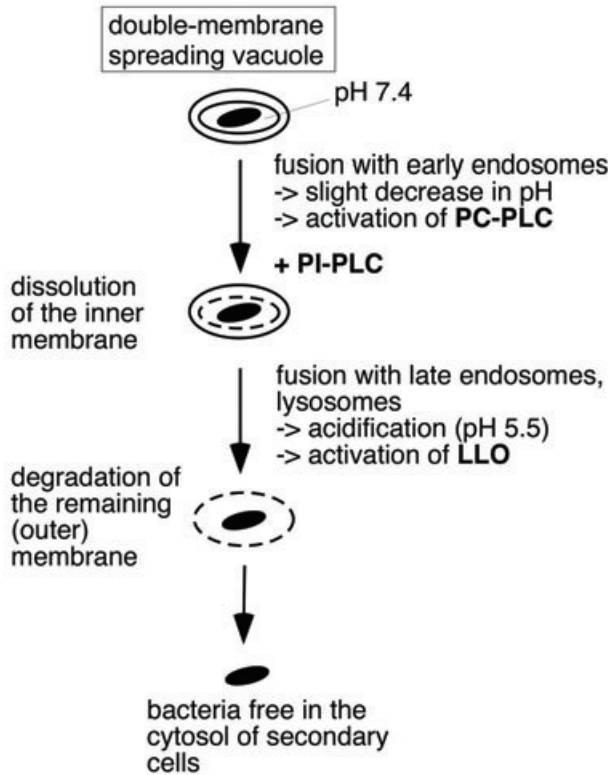
A.
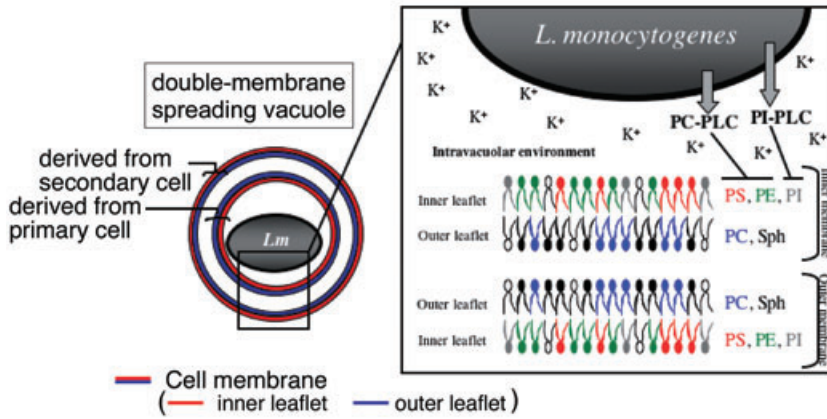
B.

Fig. 7. Model for escape of
L. monocytogenes from spreading vacuoles in
murine cells.
A. Schematic representation of the
double-membrane spreading vacuole formed
upon cell-to-cell spread. The phospholipid
composition of the inner and outer leaflets is
based on the general features of phospholipid
asymmetry in eukaryotic cells (Zwaal *et al.*,
1975). The high potassium concentration in
the internal compartment and the presence of
substrates for phospholipase activity facilitate
PI-PLC/PC-PLC dissolution of the inner
membrane. PE, phosphatidylethanolamine;
PS, phosphatidylserine; PI,
phosphatidylinositol; PC, phosphatidylcholine;
Sph, sphingomyelin.
B. Schematic representation of bacterial
escape from double-membrane spreading
vacuoles. Following cell-to-cell spread, the
double-membrane vacuole fuses with early
endosomes. Upon slight decrease in pH,
PC-PLC is activated (Marquis and Hager,
2000; Yeung *et al.*, 2005) and, together with
PI-PLC, facilitates dissolution of the inner
membrane of the spreading vacuole. Upon
further acidification, LLO mediates disruption
of the outer membrane. Free in the cytosol,
bacteria initiate intracellular replication.

for primary vacuolar escape, iLLO bacteria successfully escaped secondary spreading vacuoles as indicated by the formation of plaques in the heterologous plaquing assay (Fig. 6). This result not only supports our model for secondary vacuole escape in macrophages, but also indicates that PI-PLC and PC-PLC are sufficient to allow escape of bacteria from double-membrane spreading vacuoles formed upon cell-to-cell spread from human macrophages to human epithelial cells. As PC-PLC has been shown to mediate vacuolar lysis in the absence of LLO during infection of human epithelial cells (Marquis *et al.*, 1995; Gründling *et al.*, 2003), we predicted that PC-PLC alone would be sufficient to allow escape from

U937:Hep2 heterologous spreading vacuoles. However, we did not observe plaques in the heterologous plaquing assay using ΔPI-PLC iLLO bacteria (Fig. 6C). One explanation may be that the membrane composition of U937 cells differs sufficiently from mBMDM and dissolution of the inner membrane of the heterologous spreading vacuole requires the synergistic activity of both phospholipases. It is also possible that PC-PLC is able to dissolve the U937 inner membrane, but is then not sufficient to mediate lysis of the outer membrane at a high frequency. Again, overexpression of PC-PLC alone may overcome the inability of ΔPI-PLC iLLO bacteria to escape from heterologous secondary vacuoles.

Table 4. Strains used in this study.

Strains	Genotype	Reference
L. monocytogenes		
10403S	Wild-type strain	Bishop and Hinrichs (1987)
DP-L2161	10403S Δ*hly*	Jones and Portnoy (1994)
DP-L3078	10403S Δ*actA*	Skoble *et al.* (2000)
DP-L2317	10403S Δ*hly* Δ*plcA*	Marquis *et al.* (1995)
DP-L2318	10403S Δ*hly* Δ*plcB*	Marquis *et al.* (1995)
DP-L1936 (ΔPLCs)	10403S Δ*plcA* Δ*plcB*	Smith *et al.* (1995)
DP-L2319	10403S Δ*hly* Δ*plcA* Δ*plcB*	D. Portnoy
DH-L1239 (iLLO)	DP-L2161 i-*hly* (LIV3)	This study
DH-L1256	DP-L3078 Δ*hly*	This study
DH-L1257 (Δ*actA* iLLO)	DH-L1256 i-*hly* (LIV3)	This study
DH-L1382 (ΔPLCs iLLO)	DP-L2319 i-*hly* (LIV3)	This study
DH-L1383 (ΔPI-PLC iLLO)	DP-L2317 i-*hly* (LIV3)	This study
DH-L1384 (ΔPC-PLC iLLO)	DP-L2318 i-*hly* (LIV3)	This study
E. coli		
XL1-Blue	(F′ *proAB lacI*^{q}Δ(*lacZ*)M15 Tn*10*) *recA1, end A1, gyrA96, thi-1, hsdR17, supE, relA1, lac*	Stratagene
CLG190	F′ *proAB lacI*^{q}Δ(*malF*)3 Δ(*phoA*) PvuII *phoR* Δ (*lac*)X74 Δ(*ara leu*)7697 *araD*139 *galE galK pcnB zad*::Tn*10 recA;* Str^r	D. Boyd
DH-E447	pAH12 in XL1-Blue	A. Haraga
DH-E898	pPL3 in XL1-Blue	Gründling *et al.* (2004)
DH-E1385	pPL3_Oid2 in XL1-Blue	This study
DH-E1243	pLIV3 in XL1-Blue	This study
DH-E1247	pLIV3 i-*hly* in CLG190	This study

In summary, we have shown evidence for a role of LLO and the bacterial phospholipases in dissolution of double-membrane spreading vacuoles in primary murine macrophages. We propose that membrane dissolution occurs in two steps and that bacterial escape occurs upon acidification of the vacuolar compartment (Fig. 7B). In this model, following fusion with early endosomes, PC-PLC assisted by PI-PLC mediates dissolution of the inner membrane of the spreading vacuole. Upon further acidification, LLO mediates the perforation of the outer membrane. Work is currently in progress to determine the fate of the secondary vacuole formed upon spreading and the role of acidification in vacuolar escape after cell-to-cell spread. Lastly, our data suggest that the bacterial phospholipases can substitute for LLO function during heterologous cell-to-cell spread between human macrophages and epithelial cells. The observation that LLO is dispensable for escape from secondary vacuoles formed upon spreading into human epithelial cells suggests that the vacuolar environment after degradation of the inner membrane in these cells is different from that of murine cells. It is possible that the different requirements of LLO and the phospholipases for secondary vacuole escape reflect a major difference in the phospholipid composition between human and murine cell membranes. It is also possible that the differences reside in vacuolar trafficking and the bacterial ability to control this process. Recently, Cheng *et al.* have shown that *Drosophila* cells defective in vacuolar maturation are permissive for vacuolar escape of LLO-negative bacteria (Cheng *et al.*, 2005). More importantly, our data suggest that during infection of humans, spread-ing of *L. monocytogenes* from circulating macrophages to different cell types can occur in the absence of LLO expression. As a consequence, one therapeutic strategy to prevent dissemination of *L. monocytogenes* and systemic infection in humans could be to target LLO and the two phospholipases.

Experimental procedures

Bacterial strains and growth media

All bacterial strains used in this study are listed in Table 4. *E. coli* strains were grown in Luria–Bertani (LB) medium at 37°C with shaking. *L. monocytogenes* strains were routinely grown at 37°C in brain heart infusion (BHI) broth or on BHI agar (Difco Laboratories, Detroit, MI). Fourteen to 16 h cultures of *L. monocytogenes* were usually grown in 2 ml BHI at 30°C without shaking. All bacterial strains were stored at −80°C in LB or BHI containing 40% glycerol. Antibiotics were used at the following concentrations: ampicillin at 100 μg ml^{-1}; chloramphenicol at 20 or 40 μg ml^{-1} for selection of pPL2-based vectors in *E. coli* CLG190 and XL1-Blue respectively, and 7.5 μg ml^{-1} for selection of integrated pPL2 derivatives in *L. monocytogenes*.

Construction of an inducible expression vector for conditional repression studies in L. monocytogenes

Plasmid pLIV3 is a pPL3-based vector (Gründling *et al.*, 2004) that was constructed to allow integration of a tightly regulated inducible gene expression cassette within the tRNA^{Arg} locus on the *L. monocytogenes* chromosome. Initially, the *B. subtilis* SPO-1 promoter flanked by two *E. coli lac*Oid operator sites (Oehler *et al.*, 1994) was PCR amplified from plasmid pAH12

Table 5. Primers used in this study.

Primer	Sequence	Restriction site[a]
405	5′-CTGCAGAA<u>CCACCGCGGTGG</u>ATGCATTTCAATTGTGAGCGCTCACAATTCTCTGC-3′	BstXI
276	5′-AGATAC<u>CGGCCG</u>CTAGATCACCTCCTTAAGCTTAATTGTG-3′	EagI
508	5′-ACGC<u>GTCGAC</u>TCGATCATCATAATTCTGTCTCATTATATAAC-3′	SalI
509	5′-CTGC<u>GGTACC</u>CGGTGATCCTAACTCACATTAA-3′	KpnI
205	5′-AGATAC<u>CGGCC</u>GAGAGAGGGGTGGCAAACGGTATT-3′	EagI
014	5′-GGG<u>GTCGAC</u>CTAAAAAAATTAAAAAATAAGC-3′	SalI

a. The indicated restriction endonuclease site is underlined within each oligonucleotide sequence.

using primers 405 and 276 (Table 5). The PCR fragment was digested with BstXI and EagI, and subsequently ligated into pPL3 digested with the same restriction enzymes. The resulting plasmid was named pPL3_Oid2. Next, the p60 promoter-*lacI* gene fusion was PCR amplified from pLIV1 (Dancz *et al.*, 2002) using primer pair 508/509 (Table 5). The PCR product was digested with SalI and KpnI, and subsequently ligated into pPL3_Oid2, resulting in plasmid pLIV3 (Fig. 1).

Construction of an iLLO strain (DH-L1239) suitable for conditional repression of LLO production

A DNA fragment harbouring the last 65 base pairs of the *hly* 5′ UTR region and the *hly* gene was PCR amplified from *L. monocytogenes* 10403S genomic DNA using primers 205 and 014 (Table 5). The resulting PCR fragment was digested with EagI and SalI, and subsequently ligated into plasmid pLIV3 digested with the same restriction enzymes. The resulting plasmid pLIV3 i-*hly* was verified by automated sequencing and introduced by electroporation into the LLO-negative *L. monocytogenes* strain DP-L2161 to generate strain DH-L1239 (iLLO strain). Similarly, pLIV3 i-*hly* was introduced into several LLO-negative *L. monocytogenes* strains harbouring deletions in *actA* (DH-L1256), *plcA* (DP-L2317), *plcB* (DP-L2318) or in both phospholipases (DP-L2319) to generate strains DH-L1257, DH-L1383, DH-L1384 and DH-L1382 respectively.

Haemolytic activity assay

Sixteen-hour cultures of *L. monocytogenes* were diluted 1:10 in BHI broth and grown for 5 h at 37°C. Haemolytic activity present in culture supernatants was determined as previously described (Portnoy *et al.*, 1988; Dancz *et al.*, 2002). Haemolytic units were defined as the reciprocal of the dilution of culture supernatant that yielded 50% lysis of sheep red blood cells.

Tissue culture cell growth conditions

Human-derived U937 macrophages (ATCC CRL-1593.2) and human Hep2 epithelial cells (ATCC CCL-23) were cultured in RPMI medium (Mediatech, Herndon, VA) supplemented with 10% fetal bovine serum (FBS; HyClone, Logan, UT), 2 mM glutamine, 1 mM sodium pyruvate, 100 µg ml^{-1} penicillin and streptomycin (P/S) and 55 µM β-mercaptoethanol (β-ME) (RPMI-10). For intracellular growth and cell-to-cell spread assays, host cell cultures and infections were performed in antibiotic-free RPMI-10 medium. All cell cultures were maintained at 37°C in a 5% CO_2-air atmosphere.

Preparation of mBMDM

Bone marrow cells were flushed from the femurs of BALB/c female mice with complete Dulbecco's modified Eagle's medium [DMEM (Mediatech), 7.5% FBS, 2 mM glutamine and 100 µg ml^{-1} P/S] and washed once with fresh complete DMEM medium. Cells were cultured in 100-mm-diameter Petri dishes for 3 days in bone marrow macrophage (BMMΦ) medium [DMEM supplemented with 20% FBS, 2 mM glutamine, 1 mM sodium pyruvate, 100 µg ml^{-1} P/S, 55 µM β-ME and 30% L929 cell supernatant (as a source of macrophage colony-stimulating factor)]. On day 3, fresh BMMΦ medium was added to the cultures. On day 6, BMMΦ cells were harvested by removal of DMEM media and addition of cold PBS. Recovered cells were used in experiments as a source of mBMDM.

Intracellular growth in mBMDM

Sixteen to 18 h prior to infection, 2×10^6 mBMDM were seeded in 60-mm-diameter Petri dishes containing 12-mm-diameter round glass coverslips. The following day, 16 h bacterial cultures were diluted 1:10 in fresh BHI medium and grown for an additional 2 h at 37°C with shaking. Aliquots of the mid-log phase bacterial cultures that corresponded to ~5×10^8 bacteria ml^{-1} were washed once with PBS pH 7.1 and used to infect macrophages at a multiplicity of infection (moi) of 10:1 (bacteria to host cell ratio) in RPMI-10 medium. At 30 min post infection, mBMDM were washed three times with warm PBS and fresh RPMI-10 medium was added to the cultures. At 1 h post infection, cell culture medium was removed and RPMI-10 containing 10 µg ml^{-1} gentamicin was added. For full induction, IPTG was added to the broth culture at a concentration of 0.5 mM 2 h prior to infection and was maintained during the infection at a concentration of 10 mM. The number of colony-forming units per coverslip was determined at appropriate time intervals as follows: three coverslips were removed from the culture and placed separately into conical tubes with 5 ml of sterile water. After vortexing the suspension for 15 s to lyse mBMDM cells, dilutions were plated on LB agar plates and incubated at 37°C to determine the number of intracellular bacteria. Additional coverslips were fixed and stained with Diff-Quik (DADE-Behring, Deerfield, IL) and analysed by light microscopy.

Homologous cell-to-cell spread and fluorescence microscopy assays

Cell-to-cell spread using primary CellTracker™ Blue-labelled cells (as shown in Figs 3 and 5). Sixteen to 18 h prior to infection, 4.5×10^6 primary host cells were seeded in a 100-mm-

diameter Petri dish while 1.5×10^6 secondary host cells were seeded onto 18 mm² coverslips placed in a 60-mm-diameter dish. Bacterial cultures were prepared as described for the intracellular growth assay with some modifications. For iLLO bacteria, IPTG was added to the broth culture at a final concentration of 0.5 mM 5 min prior to the end of the 2 h incubation at 37°C. Subsequent steps of infection were performed in the absence of IPTG unless otherwise indicated. Aliquots of ~5×10^8 bacteria ml⁻¹ were washed twice with PBS and used to infect monolayers of primary host cells at a moi of 1:1 for wild-type or 30:1 for iLLO bacteria in RPMI-10 medium in the absence of β-ME. At 30 min post infection, primary infected host cells were washed three times with PBS, and β-ME-free, serum-free RPMI medium containing 10 µM CellTracker™ Blue (CTB #C-2110; Molecular Probes, Eugene, OR) was added to differentially label primary host cells. After 30 min incubation (e.g. 1 h post infection), CellTracker™ Blue-labelled cells were washed three times with PBS and fresh RPMI-10 medium containing 10 µg ml⁻¹ gentamicin was added to the cultures. At 3 h (for wild-type) or at 5.5 h (for any iLLO-derived strains) post infection, CellTracker™ Blue-labelled cells were detached with cold PBS, counted and added to a secondary monolayer of unlabelled host cells at a moi of 3:5 (primary host cell to secondary host cell ratio) in the presence of 10 µg ml⁻¹ gentamicin. At 4 h post secondary infection, cells were fixed with 3.2% paraformaldehyde for 15 min at room temperature, or 14–16 h at 4°C and prepared for fluorescence microscopy. Fixed samples were washed three times with TBS-TX (25 mM Tris-HCl pH 8.0, 150 mM NaCl, 0.1% Triton X-100) before subsequent incubations with primary and secondary antibodies. Coverslips were first incubated with a rabbit polyclonal antibody against *L. monocytogenes* (Difco). Coverslips were then rinsed with TBS-TX and treated with fluorescein isothiocyanate (FITC)-conjugated donkey anti-rabbit IgG (Jackson ImmunoResearch, West Grove, PA) together with Texas Red-X phalloidin (Molecular Probes) for labelling F-actin. Specimens were mounted for microscopy using Vectashield mounting medium (Vector Laboratories, Burlingame, CA) and analysed by fluorescence microscopy for visualization of FITC, CTB and Texas-Red. Images were acquired using MetaMorph software (Molecular Devices, Downingtown, PA). For each acquisition, a Z-series was obtained and the collected Z-stack was merged into one plane using the 'Stack Arithmetic: Maximum' command of MetaMorph. Appropriate colours were assigned to each fluorescent image (blue for CTB, green for FITC and red for Texas-Red). The colour images were scaled and ultimately overlaid using the 'Overlay' command of MetaMorph.

Cell-to-cell spread with secondary CellTracker™ Blue-labelled cells (as shown in Fig. 4). Labelling of secondary host cells with CellTracker™ Blue was performed as follows: 2 h prior to secondary infection, β-ME-free, serum-free RPMI medium containing 10 µM CellTracker™ Blue was added to the culture. After 30 min incubation, CellTracker™ Blue-labelled cells were washed three times with PBS and fresh RPMI-10 medium was added to the cultures. Primary and secondary infections were performed as described above except that primary cells were left unstained.

Labelling of secondary host cells with BSA-gold and electron microscopy procedures

To differentiate between primary and secondary cells in electron microscopy, secondary host cells were labelled with colloidal gold particles prior to infection. First, 20 nm colloidal gold particles (G1652, Sigma, St Louis, MO) were coated with bovine serum albumin (BSA Fraction V, A9647, Sigma) following a protocol for adsorption of proteins to colloidal gold particles (Slot and Geuze, 1985). Briefly, the colloidal gold particle solution was adjusted to pH 7.0 prior to BSA addition to a concentration of 0.2%. Following a 10 min incubation at room temperature with stirring, the gold particle-protein complex was centrifuged at 10 000 *g* in a Beckman ultracentrifuge (Ti40 rotor) for 1 h at 4°C. The BSA-gold pellet equivalent to a 25 ml initial particle suspension was resuspended in 100 µl of PBS and store at 4°C. For labelling of host cells, BSA-gold was adjusted to an $OD_{520} = 4$ in RPMI-10 medium and added to secondary host cells for 40 min at 37°C. BSA-gold labelled cells were washed three times with warm PBS and fresh RPMI-10 medium was added to the culture. Prior to secondary infection, BSA-gold labelled cells were washed once with warm RPMI-10 media to remove any free BSA-gold particles. This procedure resulted exclusively in the labelling of secondary host cells with colloidal gold beads. Primary and secondary infections were performed as described for the cell-to-cell spread assay. At 4 h post secondary infection, cells were fixed for 1 h in 0.1 M sodium cacodylate buffer, 2% paraformaldehyde and 2.5% glutaraldehyde and incubated in 0.1 M sodium cacodylate buffer 14–16 h at 4°C. A standard protocol was used for the preparation of samples for electron microscopy. Briefly, cells were fixed with 1% Osmiumtetroxide/ 1.5% Potassiumferrocyanide, dehydrated in graded solutions of ethanol, passed through propylene oxide and embedded in epon resin. Sections of 80–90 nm thick were stained with uranyl acetate and lead citrate or in lead citrate only and examined by transmission electron microscopy.

Heterologous cell-to-cell spread from human macrophages to human epithelial cells

Sixteen to 18 h prior to infection, Hep2 cells ($3–4 \times 10^5$) were seeded in each well of a 6 well dish. Forty-eight hours prior to primary infection, human U937 macrophage cells (1×10^6 cells ml⁻¹) were differentiated by incubation with 0.018 µM phorbol myristate acetate (PMA, Sigma). After a 36 h incubation, adherent cells were detached with PBS and 4×10^6 cells were seeded in 60-mm-diameter tissue culture dishes. Incubation prior to infection was performed in RPMI-10 medium containing 0.018 µM PMA. The day of the infection, the supernatant was carefully removed and fresh RPMI-10 without PMA was added to the culture and maintained for at least 1 h prior to infection. Primary infection of U937 cells with iLLO bacteria was performed as described for the cell-to-cell spread assay with some modifications. Briefly, U937 cells were infected at a moi of 50:1 (bacteria per host cell ratio). At 30 min post infection, cells were washed three times with PBS and fresh RPMI-10 medium added. At 1 h post infection, fresh RPMI-10 containing 20 µg ml⁻¹ gentamicin was added to the cultures. At 5.5 h post infection, cells were detached with cold PBS and 4×10^5 infected U937 cells (representing a total of $1–2 \times 10^6$ bacteria) were placed on monolayers of Hep2 cells in the presence of 30 µg ml⁻¹ gentamicin and in the absence of IPTG. Monolayers were overlaid 3 h following secondary infection with an agarose-medium mixture containing 30 µg ml⁻¹ gentamicin without IPTG. At 96 h post infection a second agarose-medium overlay containing 187 µg ml⁻¹ neutral red, 30 µg ml⁻¹ gentamicin in 1× DMEM was applied to the

samples. Twenty-four to 48 h later, plaques were visualized by scanning plates to digital images.

Acknowledgements

References

Agaisse, H., Burrack, L.S., Philips, J.A., Rubin, E.J., Perrimon, N., and Higgins, D.E. (2005) Genome-wide RNAi screen for host factors required for intracellular bacterial infection. *Science* **309:** 1248–1251.

Beron, W., Alvarez-Dominguez, C., Mayorga, L., and Stahl, P.D. (1995) Membrane trafficking along the phagocytic pathway. *Trends Cell Biol* **5:** 100–104.

Birmingham, C.L., Smith, A.C., Bakowski, M.A., Yoshimori, T., and Brumell, J.H. (2006) Autophagy controls *Salmonella* infection in response to damage to the *Salmonella*-containing vacuole. *J Biol Chem* **281:** 11374–11383.

Bishop, D.K., and Hinrichs, D.J. (1987) Adoptive transfer of immunity to *Listeria monocytogenes*. The influence of *in vitro* stimulation on lymphocyte subset requirements. *J Immunol* **139:** 2005–2009.

Calderon, R.O., and DeVries, G.H. (1997) Lipid composition and phospholipid asymmetry of membranes from a Schwann cell line. *J Neurosci Res* **49:** 372–380.

Camilli, A., Goldfine, H., and Portnoy, D.A. (1991) *Listeria monocytogenes* mutants lacking phosphatidylinositol-specific phospholipase C are avirulent. *J Exp Med* **173:** 751–754.

Camilli, A., Tilney, L.G., and Portnoy, D.A. (1993) Dual roles of *plcA. Listeria monocytogenes* pathogenesis. *Mol Microbiol* **8:** 143–157.

Cheng, L.W., Viala, J.P., Stuurman, N., Wiedemann, U., Vale, R.D., and Portnoy, D.A. (2005) Use of RNA interference in *Drosophila* S2 cells to identify host pathways controlling compartmentalization of an intracellular pathogen. *Proc Natl Acad Sci USA* **102:** 13646–13651.

Cossart, P. (2000) Actin-based motility of pathogens: the Arp2/3 complex is a central player. *Cell Microbiol* **2:** 195–205.

Dancz, C.E., Haraga, A., Portnoy, D.A., and Higgins, D.E. (2002) Inducible control of virulence gene expression in *Listeria monocytogenes*: temporal requirement of listeriolysin O during intracellular infection. *J Bacteriol* **184:** 5935–5945.

Domann, E., Wehland, J., Rohde, M., Pistor, S., Hartl, M., Goebel, W., *et al.* (1992) A novel bacterial virulence gene in *Listeria monocytogenes* required for host cell microfilament interaction with homology to the proline-rich region of vinculin. *EMBO J* **11:** 1981–1990.

Dramsi, S., Biswas, I., Maguin, E., Braun, L., Mastroeni, P., and Cossart, P. (1995) Entry of *Listeria monocytogenes* into hepatocytes requires expression of InlB, a surface protein of the internalin multigene family. *Mol Microbiol* **16:** 251–261.

Dramsi, S., Levi, S., Triller, A., and Cossart, P. (1998) Entry of *Listeria monocytogenes* into neurons occurs by cell-to-cell spread: an *in vitro* study. *Infect Immun* **66:** 4461–4468.

Drevets, D.A. (1999) Dissemination of *Listeria monocytogenes* by infected phagocytes. *Infect Immun* **67:** 3512–3517.

Drevets, D.A., and Leenen, P.J. (2000) Leukocyte-facilitated entry of intracellular pathogens into the central nervous system. *Microbes Infect* **2:** 1609–1618.

Drevets, D.A., Sawyer, R.T., Potter, T.A., and Campbell, P.A. (1995) *Listeria monocytogenes* infects human endothelial cells by two distinct mechanisms. *Infect Immun* **63:** 4268–4276.

Drevets, D.A., Jelinek, T.A., and Freitag, N.E. (2001) *Listeria monocytogenes*-infected phagocytes can initiate central nervous system infection in mice. *Infect Immun* **69:** 1344–1350.

Gaillard, J.L., Berche, P., Mounier, J., Richard, S., and Sansonetti, P. (1987) *In vitro* model of penetration and intracellular growth of *L. monocytogenes* in human enterocyte-like cell line Caco-2. *Infect Immun* **55:** 2822–2829.

Gedde, M.M., Higgins, D.E., Tilney, L.G., and Portnoy, D.A. (2000) Role of listeriolysin O in cell-to-cell spread of *Listeria monocytogenes*. *Infect Immun* **68:** 999–1003.

Geoffroy, C., Raveneau, J., Beretti, J., Lecroisey, A., Vazquez-Boland, J., Alouf, J.E., and Berche, P. (1991) Purification and characterization of an extracellular 29-kilodalton phospholipase C from *Listeria monocytogenes*. *Infect Immun* **59:** 2382–2388.

Goldfine, H., and Knob, C. (1992) Purification and characterization of *Listeria monocytogenes* phosphatidylinositol-specific phospholipase C. *Infect Immun* **60:** 4059–4067.

Goldfine, H., Johnston, N.C., and Knob, C. (1993) Nonspecific phospholipase C of *Listeria monocytogenes*: activity on phospholipids in Triton X-100-mixed micelles and in biological membranes. *J Bacteriol* **175:** 4298–4306.

Gouin, E., Welch, M.D., and Cossart, P. (2005) Actin-based motility of intracellular pathogens. *Curr Opin Microbiol* **8:** 35–45.

Greiffenberg, L., Goebel, W., Kim, K.S., Weiglein, I., Bubert, A., Engelbrecht, F., *et al.* (1998) Interaction of *Listeria monocytogenes* with human brain microvascular endothelial cells: InlB-dependent invasion, long-term intracellular growth, and spread from macrophages to endothelial cells. *Infect Immun* **66:** 5260–5267.

Gruenberg, J., and Maxfield, F.R. (1995) Membrane transport in the endocytic pathway. *Curr Opin Cell Biol* **7:** 552–563.

Gründling, A., Gonzalez, M.D., and Higgins, D.E. (2003) Requirement of the *Listeria monocytogenes* broad-range phospholipase PC-PLC during infection of human epithelial cells. *J Bacteriol* **185:** 6295–6307.

Gründling, A., Burrack, L.S., Archie Bouwer, H.G., and Higgins, D.E. (2004) *Listeria monocytogenes* regulates flagellar motility gene expression through MogR, a transcriptional repressor required for virulence. *Proc Natl Acad Sci USA* **101:** 12318–12323.

Hernandez, L.D., Pypaert, M., Flavell, R.A., and Galan, J.E. (2003) A *Salmonella* protein causes macrophage cell death by inducing autophagy. *J Cell Biol* **163:** 1123–1131.

Join-Lambert, O.F., Ezine, S., Le Monnier, A., Jaubert, F., Okabe, M., Berche, P., and Kayal, S. (2005) *Listeria monocytogenes*-infected bone marrow myeloid cells promote bacterial invasion of the central nervous system. *Cell Microbiol* **7:** 167–180.

Jones, S., and Portnoy, D.A. (1994) Characterization of *Listeria monocytogenes* pathogenesis in a strain expressing perfringolysin O in place of listeriolysin O. *Infect Immun* **62:** 5608–5613.

Kocks, C., Gouin, E., Tabouret, M., Berche, P., Ohayon, H., and Cossart, P. (1992) *L. monocytogenes*-induced actin assembly requires the *actA* gene product, a surface protein. *Cell* **68:** 521–531.

Kuhn, M., Kathariou, S., and Goebel, W. (1988) Hemolysin supports survival but not entry of the intracellular bacterium *Listeria monocytogenes*. *Infect Immun* **56:** 79–82.

Lauer, P., Chow, M.Y.N., Loessner, M.J., Portnoy, D.A., and Calendar, R. (2002) Construction, characterization, and use of two *Listeria monocytogenes* site-specific phage integration vectors. *J Bacteriol* **184:** 4177–4186.

Lorber, B. (1997) Listeriosis. *Clin Infect Dis* **24:** 1–9.

Mackaness, G.B. (1962) Cellular resistance to infection. *J Exp Med* **116:** 381–406.

Marquis, H., and Hager, E.J. (2000) pH-regulated activation and release of a bacteria-associated phospholipase C during intracellular infection by *Listeria monocytogenes*. *Mol Microbiol* **35:** 289–298.

Marquis, H., Doshi, V., and Portnoy, D.A. (1995) The broad-range phospholipase C and a metalloprotease mediate listeriolysin O-independent escape of *Listeria monocytogenes* from a primary vacuole in human epithelial cells. *Infect Immun* **63:** 4531–4534.

Montes, L.R., Goni, F.M., Johnston, N.C., Goldfine, H., and Alonso, A. (2004) Membrane fusion induced by the catalytic activity of a phospholipase C/sphingomyelinase from *Listeria monocytogenes*. *Biochemistry* **43:** 3688–3695.

Mounier, J., Ryter, A., Coquis-Rondon, M., and Sansonetti, P.J. (1990) Intracellular and cell-to-cell spread of *Listeria monocytogenes* involves interaction with F-actin in the enterocytelike cell line Caco-2. *Infect Immun* **58:** 1048–1058.

Oehler, S., Amouyal, M., Kolkhof, P., von Wilcken-Bergmann, B., and Muller-Hill, B. (1994) Quality and position of the three *lac* operators of *E. coli* define efficiency of repression. *EMBO J* **13:** 3348–3355.

Ogawa, M., Yoshimori, T., Suzuki, T., Sagara, H., Mizushima, N., and Sasakawa, C. (2005) Escape of intracellular *Shigella* from autophagy. *Science* **307:** 727–731.

Pitt, A., Mayorga, L.S., Stahl, P.D., and Schwartz, A.L. (1992) Alterations in the protein composition of maturing phagosomes. *J Clin Invest* **90:** 1978–1983.

Portnoy, D.A., Jacks, P.S., and Hinrichs, D.J. (1988) Role of hemolysin for the intracellular growth of *Listeria monocytogenes*. *J Exp Med* **167:** 1459–1471.

Pron, B., Boumaila, C., Jaubert, F., Berche, P., Milon, G., Geissmann, F., and Gaillard, J.L. (2001) Dendritic cells are early cellular targets of *Listeria monocytogenes* after intestinal delivery and are involved in bacterial spread in the host. *Cell Microbiol* **3:** 331–340.

Pust, S., Morrison, H., Wehland, J., Sechi, A.S., and Herrlich, P. (2005) *Listeria monocytogenes* exploits ERM protein functions to efficiently spread from cell to cell. *EMBO J* **24:** 1287–1300.

Sanger, J.M., Sanger, J.W., and Southwick, F.S. (1992) Host cell actin assembly is necessary and likely to provide the propulsive force for intracellular movement of *Listeria monocytogenes*. *Infect Immun* **60:** 3609–3619.

Sidhu, G., Li, W., Laryngakis, N., Bishai, E., Balla, T., and Southwick, F. (2005) Phosphoinositide 3-kinase is required for intracellular *Listeria monocytogenes* actin-based motility and filopod formation. *J Biol Chem* **280:** 11379–11386.

Skoble, J., Portnoy, D.A., and Welch, M.D. (2000) Three regions within ActA promote Arp2/3 complex-mediated actin nucleation and *Listeria monocytogenes* motility. *J Cell Biol* **150:** 527–538.

Slot, J.W., and Geuze, H.J. (1985) A new method of preparing gold probes for multiple-labeling cytochemistry. *Eur J Cell Biol* **38:** 87–93.

Smith, G.A., Marquis, H., Jones, S., Johnston, N.C., Portnoy, D.A., and Goldfine, H. (1995) The two distinct phospholipases C of *Listeria monocytogenes* have overlapping roles in escape from a vacuole and cell-to-cell spread. *Infect Immun* **63:** 4231–4237.

Vazquez-Boland, J., Kocks, C., Dramsi, S., Ohayon, H., Geoffroy, C., Mengaud, J., and Cossart, P. (1992) Nucleotide sequence of the lecithinase operon of *Listeria monocytogenes* and possible role of lecithinase in cell-to-cell spread. *Infect Immun* **60:** 219–230.

Vazquez-Boland, J.A., Kuhn, M., Berche, P., Chakraborty, T., Dominguez-Bernal, G., Goebel, W., *et al.* (2001) *Listeria* pathogenesis and molecular virulence determinants. *Clin Microbiol Rev* **14:** 584–640.

Yeung, P.S., Zagorski, N., and Marquis, H. (2005) The metalloprotease of *Listeria monocytogenes* controls cell wall translocation of the broad-range phospholipase C. *J Bacteriol* **187:** 2601–2608.

Zwaal, R.F., Roelofsen, B., Comfurius, P., and van Deenen, L.L. (1975) Organization of phospholipids in human red cell membranes as detected by the action of various purified phospholipases. *Biochim Biophys Acta* **406:** 83–96.